

Identification of a New Form of Electron Coupling in $\text{Bi}_2\text{Sr}_2\text{CaCu}_2\text{O}_8$ Superconductor by Laser-Based Angle-Resolved Photoemission

Wentao Zhang¹, Guodong Liu¹, Lin Zhao¹, Haiyun Liu¹, Jianqiao Meng¹, Xiaoli Dong¹, Wei Lu¹, J. S. Wen², Z. J. Xu², G. D. Gu², T. Sasagawa³, Guiling Wang⁴, Yong Zhu⁵, Hongbo Zhang⁴, Yong Zhou⁴, Xiaoyang Wang⁵, Zhongxian Zhao¹, Chuangtian Chen⁵, Zuyan Xu⁴ and X. J. Zhou^{1,*}

¹National Laboratory for Superconductivity, Beijing National Laboratory for Condensed Matter Physics, Institute of Physics, Chinese Academy of Sciences, Beijing 100080, China

²Condensed Matter Physics and Materials Science Department, Brookhaven National Laboratory, Upton, New York 11973, USA

³Materials and Structures Laboratory, Tokyo Institute of Technology, Yokohama Kanagawa, Japan

⁴Laboratory for Optics, Beijing National Laboratory for Condensed Matter Physics, Institute of Physics, Chinese Academy of Sciences, Beijing 100080, China

⁵Technical Institute of Physics and Chemistry, Chinese Academy of Sciences, Beijing 100080, China

Laser-based angle-resolved photoemission measurements with super-high resolution have been carried out on an optimally-doped $\text{Bi}_2\text{Sr}_2\text{CaCu}_2\text{O}_8$ high temperature superconductor. New high energy features at ~ 115 meV and ~ 150 meV, besides the prominent ~ 70 meV one, are found to develop in the nodal electron self-energy in the superconducting state. These high energy features, which can not be attributed to electron coupling with single phonon or magnetic resonance mode, point to the existence of a new form of electron coupling in high temperature superconductors.

PACS numbers: 74.72.Hs, 74.25.Jb, 79.60.-i, 71.38.-k

The physical properties of materials are dictated by the microscopic electron dynamics that relies on the many-body effects, i.e., the interactions of electrons with other excitations, like phonons, magnons and so on. How to detect and disentangle these many-body effects is critical to understand the macroscopic physical properties and the superconductivity mechanism in high temperature superconductors. Angle-resolved photoemission spectroscopy (ARPES), as a powerful tool in probing many-body effects[1], has revealed clear evidence of electron coupling with low energy collective excitations (bosons) at an energy scale of ~ 70 meV[2, 3, 4, 5, 6, 7] in the nodal region and ~ 40 meV near the antinodal region[4, 8, 9, 10] although the nature of the bosonic modes remains under debate as to whether it is phonon[5, 6, 10] or magnetic resonance mode[3, 4, 7, 8, 11]. Recently, another high energy feature is identified in dispersion at $300\sim 400$ meV but its origin remains unclear as to whether this can be attributed to a many-body effect[12].

In this paper we report an identification of a new form of electron coupling in high temperature superconductors by taking advantage of super-high resolution vacuum ultra-violet (VUV) laser-based ARPES technique[13]. New features at energy scales of ~ 115 meV and ~ 150 meV are revealed in the electron self-energy in $\text{Bi}_2\text{Sr}_2\text{CaCu}_2\text{O}_8$ ($\text{Bi}2212$) superconductor in the superconducting state. These features can not be attributed to electron coupling with single phonon mode or magnetic resonance mode. They point to a possibility of electron coupling with some high energy excitations in high temperature superconductors.

The angle-resolved photoemission measurements have been carried out on our newly-developed VUV laser-

based angle-resolved photoemission system[13]. The photon energy of the laser is 6.994 eV with a bandwidth of 0.26 meV. The energy resolution of the electron energy analyzer (Scienta R4000) is set at 0.5 meV, giving rise to an overall energy resolution of 0.56 meV which is significantly improved from $10\sim 15$ meV from regular synchrotron radiation systems[2, 3, 4, 5, 6, 7]. The angular resolution is $\sim 0.3^\circ$, corresponding to a momentum resolution $\sim 0.004 \text{ \AA}^{-1}$ at the photon energy of 6.994 eV, more than twice improved from 0.009 \AA^{-1} at a regular photon energy of 21.2 eV for the same angular resolution. The photon flux is adjusted between 10^{13} and 10^{14} photons/second. The optimally-doped $\text{Bi}2212$ single crystals with a superconducting transition temperature $T_c=91\text{K}$ were cleaved *in situ* in vacuum with a base pressure better than 5×10^{-11} Torr.

Fig. 1a shows the raw data of photoelectron intensity as a function of energy and momentum for an optimally-doped ($\text{Bi}2212$) superconductor ($T_c=91\text{K}$) measured along the $\Gamma(0,0)$ - $Y(\pi,\pi)$ nodal direction at a temperature of 17K. By fitting momentum distribution curves (MDCs), the dispersion (Fig. 1b) and MDC width (inset of Fig. 1b) are quantitatively extracted from Fig. 1a. One can see an obvious kink in dispersion near 70 meV (Fig. 1a and b) and a drop in the MDC width (inset of Fig. 1b), similar to those reported before[2, 3, 4, 5, 6, 7] but with much improved clarity. It is generally agreed that this 70 meV feature originates from a coupling of electrons with a collective boson mode. When coming to the nature of the boson mode, it remains under debate whether it is phonon[5, 6] or magnetic resonance mode[3, 4, 7].

The real part of the electron self-energy can be ex-

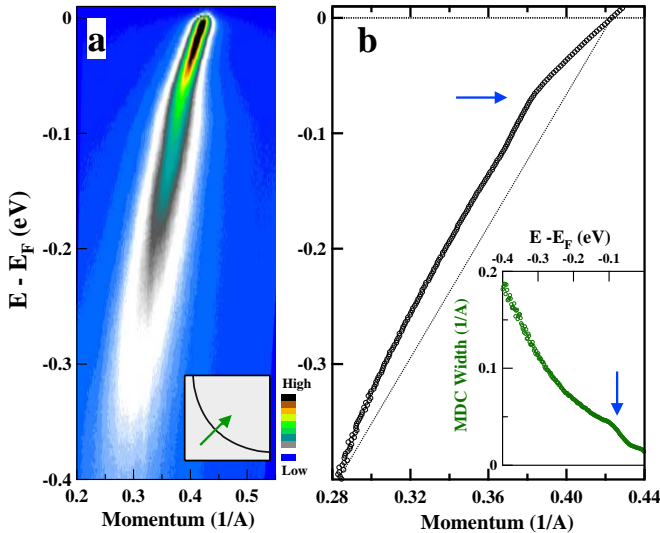


FIG. 1: Electron dynamics of optimally-doped Bi2212 ($T_c=91\text{K}$) measured along the $\Gamma(0,0)$ - $Y(\pi,\pi)$ nodal direction at 17K. (a). Raw image showing photoelectron intensity (represented by false color) as a function of energy and momentum. The inset shows the location of the momentum cut in the Brillouin zone; (b). Nodal dispersion extracted from Fig. 1a by fitting MDCs. The dotted line connecting the two energy positions in the dispersion at the Fermi energy and -0.4eV is an empirical bare band for extracting the effective real part of self-energy in Fig. 2b. The inset shows the corresponding MDC width (Full-Width-at-Half-Maximum, FWHM).

tracted from the dispersion given that the bare band dispersion is known which can be determined in a number of ways but still without consensus[14, 15]. To identify fine features in the electron self-energy and study their relative change with temperature, it is reasonable to assume a featureless bare band for the nodal dispersion within a small energy window near the Fermi energy. In this case, the fine features manifest themselves either as peaks or curvature changes in the “effective self-energy”[15]. As shown in Fig. 1b, we choose here a straight line connecting two energy positions in the dispersion at the Fermi energy and -0.4eV as the empirical bare band. The resultant effective real part of electron self-energy is shown in Fig. 2b. Also shown in Fig. 2 are dispersions (Fig. 2a) along several other cuts in the Brillouin zone (inset of Fig. 2a) and the corresponding effective electron self-energy (Fig. 2b).

With much improved precision of data, one can identify clearly several features in the electron self-energy, as shown in Fig. 2b. The most pronounced feature is the peak at $\sim 70\text{meV}$ that gives rise to the kink in dispersion seen here and before[2, 3, 4, 5, 6, 7]. In addition, at higher energies, two new features can be identified clearly as a valley at $\sim 115\text{meV}$ and a cusp at $\sim 150\text{meV}$. Signature of a fine feature near 94meV is also visible, particularly for the two cuts close to nodal region (cuts

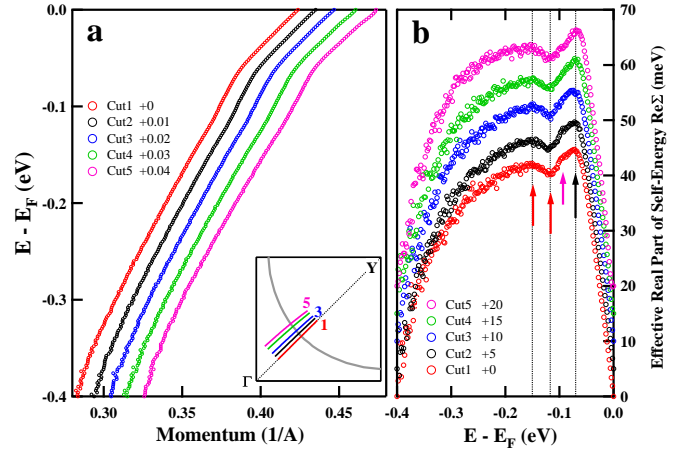


FIG. 2: Momentum dependence of dispersions(a) and corresponding effective real part of electron self-energy (b). The inset of Fig. 2a shows the location of momentum cuts in the Brillouin zone. The effective self-energy in Fig. 2b is obtained by taking the straight line connecting two positions in dispersion at the Fermi energy and -0.4eV as a bare band. The arrows in Fig. 2b mark fine features at $\sim 70\text{meV}$, 115meV , and 150meV , and a possible feature near 94meV . For clarity, curves in Fig. 2a is offset along the momentum axis while curves in Fig. 2b is offset along the vertical axis; the offset values are given in the legends.

1 and 2). Between the Fermi level and 70meV , we have also observed hints of possible low-energy features which are however very subtle and need further measurements to pin them down. We note that the bare band selection has little effect on the identification of these fine features and their energy position as we have checked by trying other straight lines as empirical bare bands. Particularly, the two new features at 115meV and 150meV , together with the 70meV peak, are robust (as also shown in Fig. 4 below) and persist in a rather large momentum space near the nodal region.

The nodal electron dynamics undergoes a dramatic evolution with temperature and superconducting transition, as indicated by the temperature dependence of the nodal dispersion (Fig. 3a) and scattering rate (Fig. 3b). In Fig. 3a, a quantitative momentum variation with temperature at four typical energy positions (the Fermi level, -0.07eV , -0.2eV and -0.3eV) is plotted in the upper-left inset and some representative MDCs for these four energies at 17K and 128K are plotted in the bottom-right inset. Over the temperature range of the measurement, the dispersion change with temperature spreads over an energy range of $0\sim 300\text{meV}$ within which the dispersion renormalization gets stronger with decreasing temperature.

An unexpected finding is the Fermi momentum shift with temperature (Fig. 3a and top-left inset) which increases with increasing temperature in the superconduct-

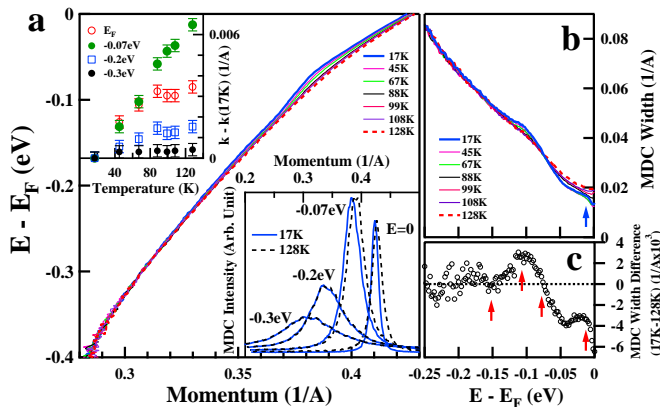


FIG. 3: Temperature dependence of the nodal MDC dispersion (a) and MDC width (b). The top-left inset of Fig. 3a plots the momentum value as a function of temperature at four typical energies: E_F (red empty circle), -0.07 eV (green solid circle), -0.2 eV (blue empty square) and -0.3 eV (black solid circle) obtained by averaging over ± 10 meV energy range. The bottom-right inset of Fig. 3a shows MDCs at these four energies measured at 17K (solid line) and 128K (dashed line). (c). The difference of the MDC width between two temperatures at 17K and 128K. Arrows in Fig. 3b and c mark possible features showing up in the scattering rate.

ing state below $T_c=91$ K and then becomes nearly flat above T_c . The magnitude of the shift is small, on the order of 0.003 \AA^{-1} , and the change is monotonic. We first checked whether this could be caused by sample orientation change during heating/cooling process and feel that it is unlikely because this usually would cause a shift of overall dispersion. As shown in Fig 3a and the top-left inset, the dispersion above 300 meV shows little change with temperature. In fact, the MDCs themselves at 300 meV overlap with each other at 17K and 128K almost perfectly, as shown in the bottom-right inset of Fig. 3a. Another possibility we have checked is whether it can be caused by the thermal expansion or contraction of the sample during temperature change. This can also be excluded because with the lattice expansion with increasing temperature, one would expect a shrink of the Brillouin zone that causes the nodal Fermi momentum move to smaller value; this expected trend is just opposite to our experimental observation. Because the Fermi momentum shift with temperature is quite unusual and has not been reported before, we have repeated the measurement and reproduced the similar observation. Therefore, to the best of our effort, we think this is likely an intrinsic effect and its first observation is a result of much improved instrumental precision. Further work needs to be done to pin down this effect and understand the underlying physical origin as it suggests either a chemical potential shift or Fermi surface topology change upon entering the superconducting state.

The scattering rate shows a strong variation with tem-

perature at low energy range within $0 \sim -0.2$ eV, as shown in Fig. 3b. Interestingly, the temperature dependence is not monotonic but depends on the binding energy. Between the Fermi level and -0.07 eV, the scattering rate decreases with decreasing temperature, while it increases with decreasing temperature between -0.07 and -0.15 eV. This gives rise to an “overshoot” region extending to ~ 0.1 eV at low temperature. The change of the scattering rate with temperature can also be clearly seen in the difference between the normal and superconducting states, as plotted in Fig. 3c which depicts the difference between 17K and 128K data. Here the difference between -0.07 eV and -0.15 eV is positive while it becomes negative between E_F and -0.07 eV.

The temperature dependence of the effective real part of self-energy (Fig. 4) indicates that the new high energy features at 115 meV and 150 meV are developed in the superconducting state. Fig. 4a shows the effective real part of self-energy at various temperatures obtained from the dispersions (Fig. 3a) by selecting a common empirical bare band, i.e., a straight line connecting the Fermi energy and -0.4 eV in the dispersion at 128K. Fig. 4b shows the net temperature change of electron self-energy with respect to the normal state data at 128K, thus avoiding any ambiguity from bare band selection. It is clear in both cases that dramatic change of electron self-energy occurs in the superconducting state, with a sharpening of the ~ 70 meV feature, together with the emerging and growing of the ~ 115 meV and ~ 150 meV features. These observations are consistent with the scattering rate data where one can see the emergence of similar characteristic energy scales at ~ 150 meV, ~ 115 meV and ~ 70 meV in the superconducting state (Fig. 3c).

The identification of high energy features at 115 meV and 150 meV points to a new form of electron coupling in high temperature superconductors. These are qualitatively different from the ~ 70 meV feature which is attributed to coupling of electrons with some collective modes and such modes with comparable energy scales are available in high temperature superconductors either as phonon[5, 6] or magnetic resonance mode[3, 4, 7]. Because the energy scale of these two new features is higher than the maximum energy of phonons (~ 90 meV)[16] and magnetic resonance mode (42 meV in optimally-doped Bi2212)[17], they can not be due to electron coupling with a single phonon or magnetic resonance mode. Although the effect of the electron-boson coupling for a low-energy mode can extend to high energy in the electron self-energy, it will not generate any new features with clear curvature change, as evidenced from simulations of electron-phonon coupling using both Debye and Einstein models and confirmed in canonical electron-phonon coupling systems[18].

There are a couple of possibilities that may give rise to high energy features in the electron coupling. The first is the mode energy shift due to the opening of supercon-

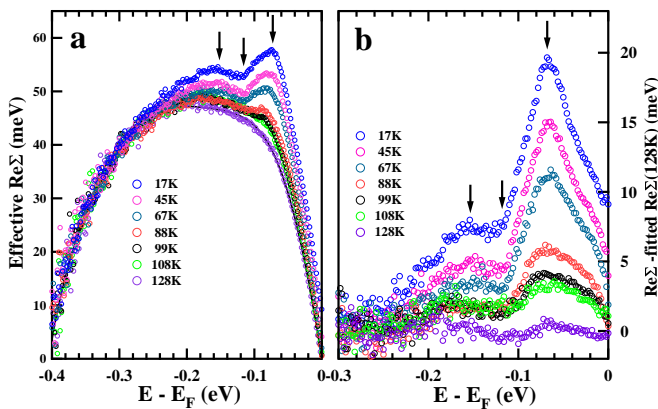


FIG. 4: (a). Temperature dependence of the effective real part of electron self-energy extracted from dispersions in Fig. 3a by taking a straight line as a bare band connecting two points at E_F and -0.4eV on the dispersion at 128K. (b). Temperature dependence of the difference between the measured self-energy in Fig. 4a and the fitted one for 128K (solid black line in Fig. 4a). The 128K self-energy is fitted by polynomials and used to reduce statistical errors.

ducting gap: the original mode position in the normal state is expected to be shifted upward by an amount on the order of the superconducting gap upon entering the superconducting state[19]. In the optimally-doped Bi2212, with the maximum d-wave superconducting gap at $\sim 35\text{meV}$, one might expect that the original $\sim 70\text{meV}$ mode be shifted to a higher energy around 105meV . However, this scenario is difficult to explain the existence of another 150meV feature, the feature at 110meV being a valley instead of a peak and the remaining strong $\sim 70\text{meV}$ feature. Another possibility is the electron coupling with multiple phonons. Usually this effect is expected to be much weaker[20] although in principle the possibility can not be totally excluded. More theoretical work are needed to verify whether such multiphonon process can produce clear features at high energy and whether such an effect is enhanced at low temperature. The third possibility is electron coupling with excitations that are already present at such high energy scales. The emergence and evolution of the 115meV and 150meV features in the electron self-energy is probably due to the redistribution of the underlying spectral function of the high energy excitations with temperature and superconducting transition. One candidate of such high energy excitations in high temperature superconductors seems to be naturally related to the spin fluctuation observed by neutron scattering, which covers a large energy range up to 200meV and exhibits strong temperature dependence[21]. Signature of such high energy coupling is also proposed from optical measurements[22]. Further theoretical work to investigate the effect of such high energy spin excitations on electron dynamics will help in clarifying such a scenario.

In conclusion, by performing high precision ARPES measurements on Bi2212, we have revealed new features at 115meV and 150meV in the electron self-energy developed in the superconducting state. They can not be attributed to electron coupling with either single phonon or magnetic resonance mode but point to the existence of a new form of electron coupling in high temperature superconductors. We hope this observation will stimulate further theoretical work to understand their origin and their role in determining anomalous physical properties of high temperature superconductors.

We acknowledge helpful discussions with J. R. Shi, T. Xiang, Z. Y. Weng and S. Kivelson. This work is supported by the NSFC, the MOST of China (973 project No: 2006CB601002, 2006CB921302), and CAS (Projects ITSNEM and 100-Talent). The work at BNL is supported by the DOE under contract No. DE-AC02-98CH10886.

*Corresponding author (XJZhou@aphy.iphy.ac.cn)

- [1] A. Damascelli et al., Rev. Mod. Phys. **75**, 473(2003); J. C. Campuzano et al., in The Physics of Superconductors, Vol. 2, edited by K. H. Bennemann and J. B. Ketterson, (Springer, 2004); X. J. Zhou et al., in Handbook of High-Temperature Superconductivity: Theory and Experiment, edited by J. R. Schrieffer, (Springer, 2007).
- [2] P. V. Bogdanov et al., Phys. Rev. Lett. **85**, 2581(2000).
- [3] P. Johnson et al., Phys. Rev. Lett. **87**, 177007(2001).
- [4] A. Kaminski et al., Phys. Rev. Lett. **86**, 1070(2001).
- [5] A. Lanzara et al., Nature (London) **412**, 510 (2001).
- [6] X. J. Zhou et al., Nature (London) **423**, 398 (2003).
- [7] A. A. Kordyuk et al., Phys. Rev. Lett. **97**, 017002 (2006).
- [8] A. D. Gromko et al., Phys. Rev. B **68**, 174520(2003).
- [9] T. K. Kim et al., Phys. Rev. Lett. **91**, 167002(2003).
- [10] T. Cuk et al., Phys. Rev. Lett. **93**, 117003(2004).
- [11] M. Eschrig and M. R. Norman, Phys. Rev. Lett. **85**, 3261 (2000).
- [12] F. Ronning et al., Phys. Rev. B **71**, 094518(2005); J. Graf et al., Phys. Rev. Lett. **98**, 067004(2007); B. P. Xie et al., Phys. Rev. Lett. **98**, 147001(2007); T. Valla et al., Phys. Rev. Lett. **98**, 167003(2007); W. Meevasana et al., Phys. Rev. B **75**, 174506(2007); J. Chang et al., Phys. Rev. B **75**, 224508(2007); D. S. Inosov et al., cond-mat/0710.3838.
- [13] G. D Liu et al., Rev. Sci. Instruments **79**, 023105 (2008).
- [14] A. A. Kordyuk et al., Phys. Rev. B **71**, 214513 (2005).
- [15] X. J. Zhou et al., Phys. Rev. Lett. **95**, 117001 (2005).
- [16] R. J. McQueeney et al., Phys. Rev. Lett. **87**, 077001 (2001).
- [17] H. He et al., Phys. Rev. Lett. **86**, 1610 (2001).
- [18] M. Hengsberger et al., Phys. Rev. B **60**, 10796 (1999).
- [19] A. W. Sandvik et al., Phys. Rev. B **69**, 094523 (2004).
- [20] S. Engelsberg and J. R. Schrieffer, Phys. Rev. **131**, 993 (1963).
- [21] H. F. Fong et al., Phys. Rev. B **61**, 14773(2000); P.-C. Dai et al., Science **284**, 1344 (1999); B. Vignolle et al., Nature Phys. **3**, 163(2007).
- [22] J. Hwang et al., Phys. Rev. B **75**, 144508(2007).